

## Study of NaCl crystallization using Infrared Thermography

P. Vázquez<sup>1\*</sup>, C. Thomachot-Schneider<sup>1</sup>, K. Mouhoubi<sup>2</sup>,  
M. Gommeaux<sup>1</sup>, G. Fronteau<sup>1</sup>, V. Barbin<sup>1</sup> and J. L. Bodnar<sup>2</sup>

<sup>1</sup>GEGENAA EA 3795, University of Reims Champagne-Ardenne, Reims (France)

<sup>2</sup>CATHERM, GRESPI EA 4694, University of Reims Champagne-Ardenne, Reims (France)

\*patricia.vazquez@univ-reims.fr

### Abstract

The Infrared Thermography (IRT) technique has been widely developed during the last years. IRT is useful to observe changes in the fields of physics and chemistry, and has turned out to be an important and indispensable non-destructive technique used for investigation of civil engineering works, with special attention to cultural heritage.

In this research IRT has been used to study the crystallization of NaCl solution droplets with different initial concentrations (3.5, 14 and 26% weight). The crystallization was induced by evaporation of the solvent (water). Tests were carried out at two temperatures (25 and 50°C). We explained how the crystallization process is observed with IRT. The variations in emissivity recorded by the IRT described distinctly the different stages of salt crystallization. IRT allowed observing three phases. In phase I the mass diffusion within the droplet and differences in concentration and volume of the solution around the crystal germs nuclei were observed. Phase II is related to the final crystallization step, with the crystal growth and the complete evaporation of the solution. Phase III describes creeping associated with efflorescence formation. This phenomenon takes place as an intermittent decrease in the IR thermosignal which can be repeated up to 100 times in a 10 minutes interval.

Different morphologies corresponded to different IRT phases. Thus, if only phases I-II are present, crystals have cubic shape or efflorescence-like

with fan-shape. If phase III occurs, efflorescence-like crystals with spherulite shape develop. These spherulites can crystallize on the substrate or on previous crystals, growing by top-supplied creeping and showing an intermittent decrease of thermosignal.

The study and comprehension of salt droplets crystallization by IRT is the first step in our research. Currently, we are testing different salt types and the response of salt crystallization in porous stones.

**Keywords:** Infrared Thermography, emissivity, creeping, NaCl, temperature

## 1 Introduction

Salt crystallization in stones is widely recognised as an important mechanism of deterioration. The knowledge of the crystallization mechanism itself is crucial to understand stone decay [1-4]. This process can exert a destructive pressure if it occurs within the porous system [5-7] or less damage, but leading to a change in the stone appearance, if crystallization takes place on the outer surface as efflorescence [1, 8, 9]. Several authors studied these processes with new and ultraprecise tools such as Environmental Scanning Electron Microscopy [3], Atomic Force Microscopy [10], X-ray Computed Tomography [11] or Nuclear Magnetic Resonance [4].

The use of Infrared thermography (IRT) has been widely developed during the last years [12] in several areas due to its non-destructive character, including civil engineering works [13, 14] with special attention to cultural heritage [15-20]. This technique allows, on the basis of a photothermal signal, studying the moisture transfer [21] and detecting defects in a material [13, 20]. There are two main methodologies in the use of IRT, the stimulated and the passive method. In the stimulated IRT, the studied object is initially in a steady state and it is artificially put in a transient state by exciting the material with an external energy source. Stimulated IRT has been widely used for detecting defects in works of art [17, 18] and recently for salt detection in stone [22]. Passive infrared thermography is used when the study case is a process which shows temperature and emissivity variations. This is the case of moisture movement [21] or salt crystallization processes [23].

Before studying crystallization within a complex system such as a porous media, it is essential to understand the IRT response of single saline solution during crystallization. In this study, we observed and analyzed the crystallization of NaCl from solution droplets with passive IR thermography. Different solution concentrations were tested at two temperature ranges. We discuss the thermosignal variations related to the crystallization processes.

## 2 Methodology

### 2.1 Principle of Infrared Thermography

Infrared thermography is a method based on the measurement of the intensity of infrared radiation emitted by materials, commonly interpreted as changes in surface temperature. For a given material Stefan-Boltzmann's law states, in a simple form, that the quantity of radiation emitted is a function of its temperature:

$$TS = \varepsilon \cdot \sigma \cdot T^4 \quad (1)$$

where TS is the thermosignal measured by the sensor (expressed in isotherm units, I.U.),  $\varepsilon$  is the emissivity of the material (dimension-less),  $\sigma$  is the Stefan-Boltzmann constant ( $\approx 5.67 \cdot 10^{-8} \text{ J} \cdot \text{s}^{-1} \cdot \text{m}^{-2} \cdot \text{K}^{-4}$ ) and T is the temperature of the material (in K).

In the present study, crystallization was produced by evaporation at two different temperatures, 25 and 50°C. The former was the laboratory condition, the latter was reached and maintained constant during the tests with a hotplate (see setup description in next section).

The acquisition system was a FLIR infrared thermography camera SC655. It works in the longwave infrared spectrum range [7.5 – 14  $\mu\text{m}$ ], which enables to investigate a temperature range from -20 to 150 °C for most common materials. The detector is an uncooled array of microbolometers that provides images of 640 x 480 pixels. The noise signal is about 40 mK. The camera was equipped with an additional macro-objective with a magnification x1.6 which gives a spatial resolution of 50  $\mu\text{m}$  / pixel.

In order not to interfere with the evaporation, all measurements were conducted in passive IRT mode. In addition, the recording of the thermosignal along the crystallization tests was done in absolute darkness to avoid the heat release from the laboratory illumination. Prior tests concluded that the optimal recording speed in this test for the IRT was 5 images per second throughout the test. The images were treated and analyzed with the ThermaCAM Researcher 2.10 software (FLIR).

### 2.2 Experimental procedure

To be ready for crystallization, a saline solution must be supersaturated. In this study, the supersaturation was produced by evaporation of the solvent. We prepared three solutions of different concentration with distilled water and NaCl (purity of > 99%, Sigma Aldrich). The concentrations of NaCl were 35, 140 and 260  $\text{g} \cdot \text{L}^{-1}$  (thereafter referred to as 3.5%, 14% and 26% weight), the latter corresponding to near-saturation. The solutions were filtered to remove any impurities. The crystallization was studied in 10  $\mu\text{L}$  droplets of each concentration. Two drops of each concentration were placed on black adhesive tape (3M), serving as a reference material, which was stuck to a glass slide. The

experimental set-up was placed inside a Plexiglas open-top box of 50 x 40 x 30 cm (Fig. 1). Inside the box, there was enough silica gel to keep a constant humidity at  $25 \pm 5\%$ . This low RH was chosen to enhance the precipitation/crystallization. In order to avoid the air flow, the open side was covered with a transparent and mate plastic film that did not interfere with the IR detection (transparent in the wavelength analyzed by the camera [24]). Hygrometers and thermocouples were set in contact with the black tape, in order to monitor the temperature and humidity every second.

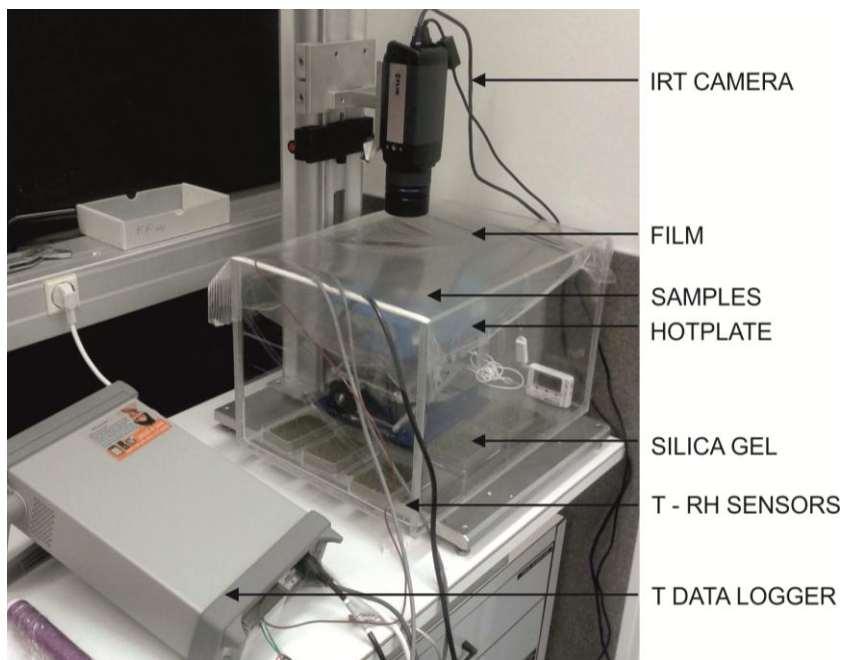


**Figure 1:** Experimental set-up.

The glass slides with the solution droplets were placed on a hot-plate. This hot-plate was switched off in the test carried out at  $25^\circ\text{C}$ , acting as support, and set at a constant temperature of  $50 \pm 1^\circ\text{C}$  in the second series of experiments, in order to accelerate the evaporation. The tests lasted until the thermosignal remained stable, once the salts were crystallized. All the equipment was plugged to a computer in order to obtain the image “in vivo” as well as the data from the thermocouples and hygrometers. In addition to whole-image observation, variations of the thermosignal during the experiments were recorded and compared between several points of the droplets and the black tape reference.

Once the droplets had crystallized, they were compared to the observed thermosignals, in order to establish the relation between some processes and crystal morphology. Photographs were taken with a stereomicroscope Olympus SZH-ILLB, with digital Tri-CCD camera (Sony, DXP 930).

Measurements of the sizes and numbers of crystals were done with the image analysis software from MicroVision Instruments.

### 3 Results and discussion

#### 3.1 Factors affecting the thermosignal in this study

Initially, this study was conceived in order to detect the exothermic process of NaCl crystallization. The observed images, processes and measurements indicated, however, a decrease in thermosignal, contrary to what was expected. Since the black adhesive tape and the droplets are at the same temperature  $\pm 0.5^{\circ}\text{C}$  (measured with thermocouples) these variations (1 - 10 I.U.) have to be due to emissivity. Distilled water and the 3M black tape have the same emissivity (0.96, [24]). Comparison between pure water droplets and the different saline solution droplets at the same temperature did not exhibit any difference in thermosignal. In spite of that, the thermosignal of the droplets was always lower than that of the black tape. In addition, differences in the thermosignal were observed within one droplet (e.g. higher thermosignal in the centre). All these emissivity differences between salt solution and tape and between different points of the same droplet are thus mainly due to shape factor and were taken into account for the interpretation of thermosignal variations in terms of crystallization processes. NaCl crystals have a reference emissivity close to 0.82 [25], that is also variable depending on several factors, such as the crystal size, if it was a single crystal or an aggregate or if the measure was made on one face or on a crystal edge.

#### 3.2 Crystallization phases

NaCl crystallization process differed in relation to temperature and concentration of the solution. The study with the IRT revealed three main phases: (I) homogeneous evaporation and crystal nucleation, (II) crystal growth driven by evaporation, and (III) crystal growth fed by solution creeping. The presence and duration of these phases depended mainly on the solution concentration and evaporation rate. Furthermore, at certain times these phases coexisted in different zones within a drop. In general, with low and medium concentration (3.5 - 14 %), crystallization followed sequences of phases I-II. In occasions an additional and weak phase III (creeping) could be found within phase II. In drops with a higher concentration (26%) phase III occurred after or instead of phase II, leading to sequences I-II-III or I-III.

**Phase I: Progressive homogenous evaporation and crystal nucleation.** At the beginning of the test, there was a marked difference in thermosignal between the droplets and the reference tape ( $\Delta\text{TS}$ ). In Figure 2a and 2e, for  $t=0$  the droplet thermosignal was clearly lower than in the black support. In Figures 3 and 4 the thermosignal differed at the

beginning of the test from 1 I.U. at 25°C to 3-10 I.U. at 50°C. Considering that temperature of droplets and support was the same (measured with thermocouples), emissivity had an important weight in the received signal,

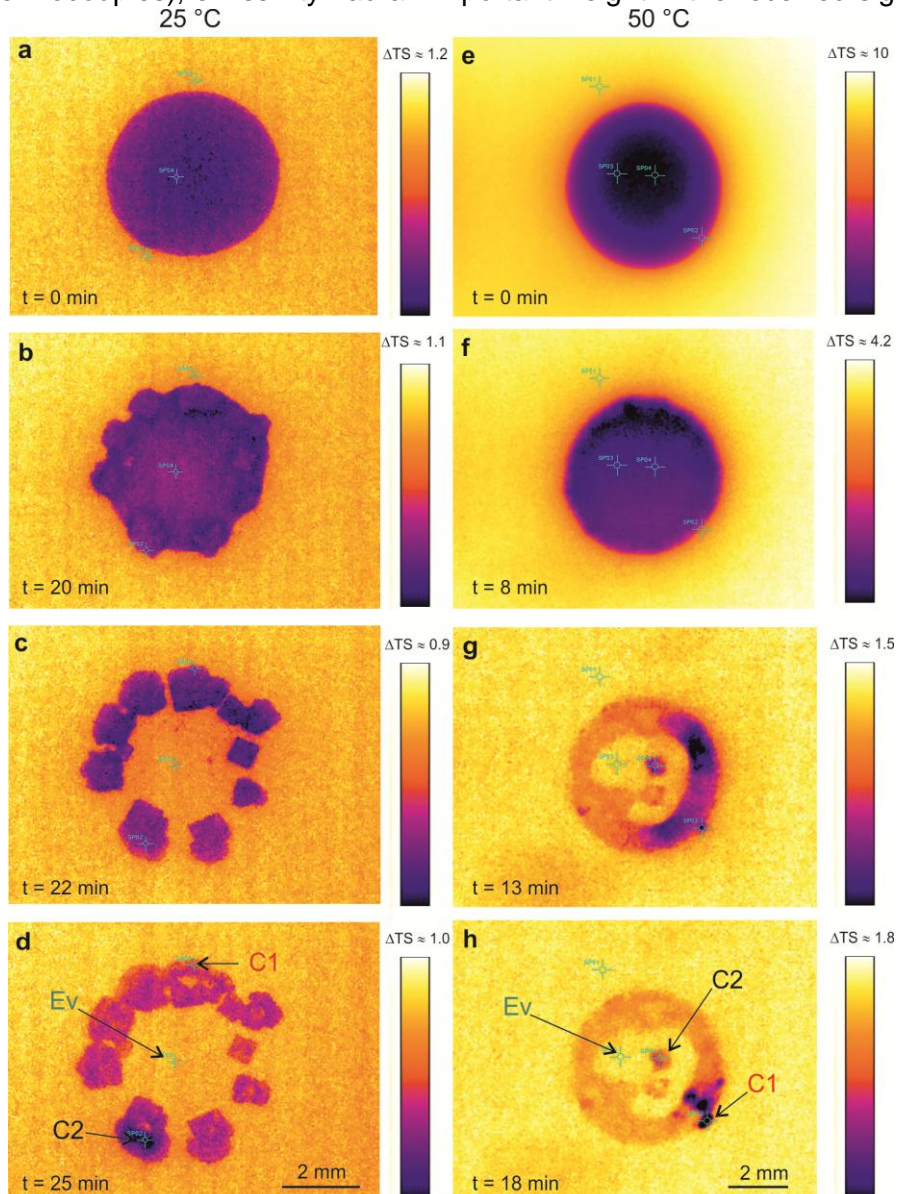


**Figure 2:** Crystallization sequence observed with IRT for two droplets at 25 °C (left) and 50 °C (right). Both droplets have 14% NaCl concentration. Marks in 2.d and 2.h correspond to profiles in figures 3 and 4. Ev: evaporation zone; C1: creeping zone 1; C2: creeping zone 2.

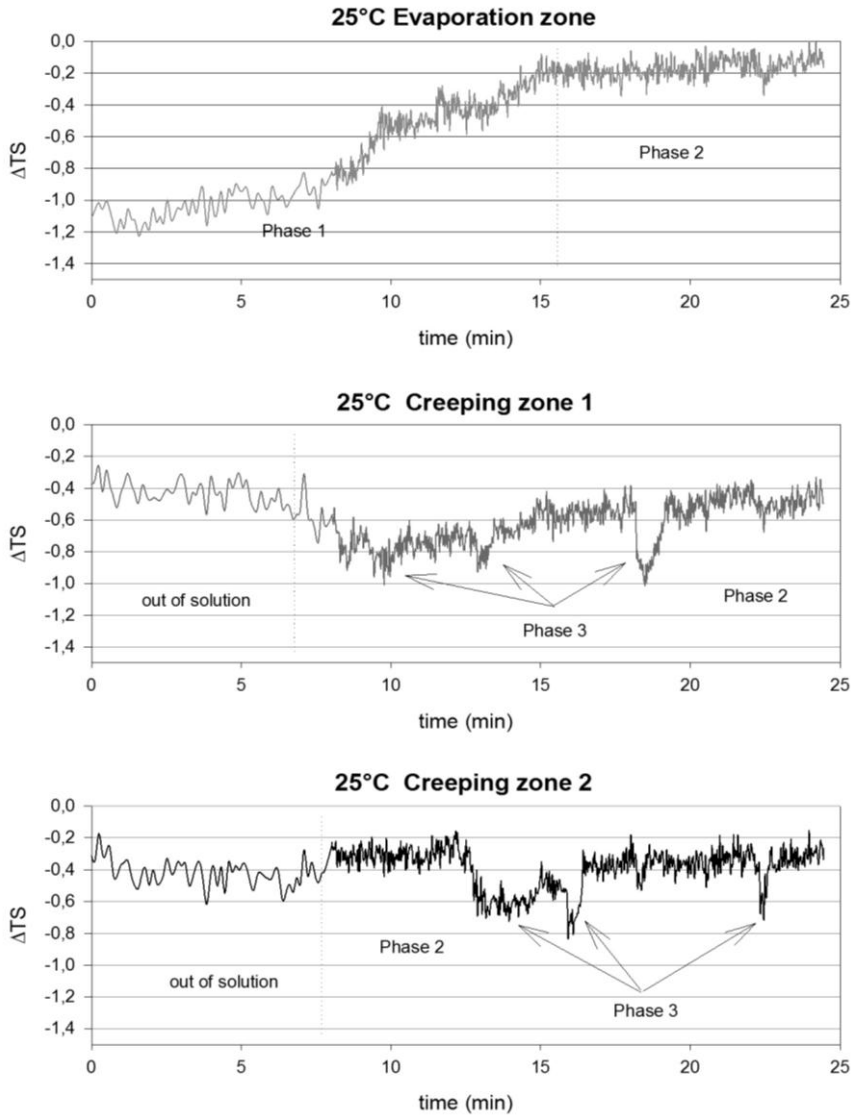


**Figure 3:** Thermosignal profiles of the crystallization sequence at 25°C. Profiles corresponded to measurements of the TS in spot mode (points indicated in Figure 2d as EV, C1 and C2). Phase I, II and III are shown. “Out of solution” corresponds to a point that is initially out of the droplet edge (reference material) but that is later reached by developing crystals. Phase III last several seconds and was more an isolated phenomena.

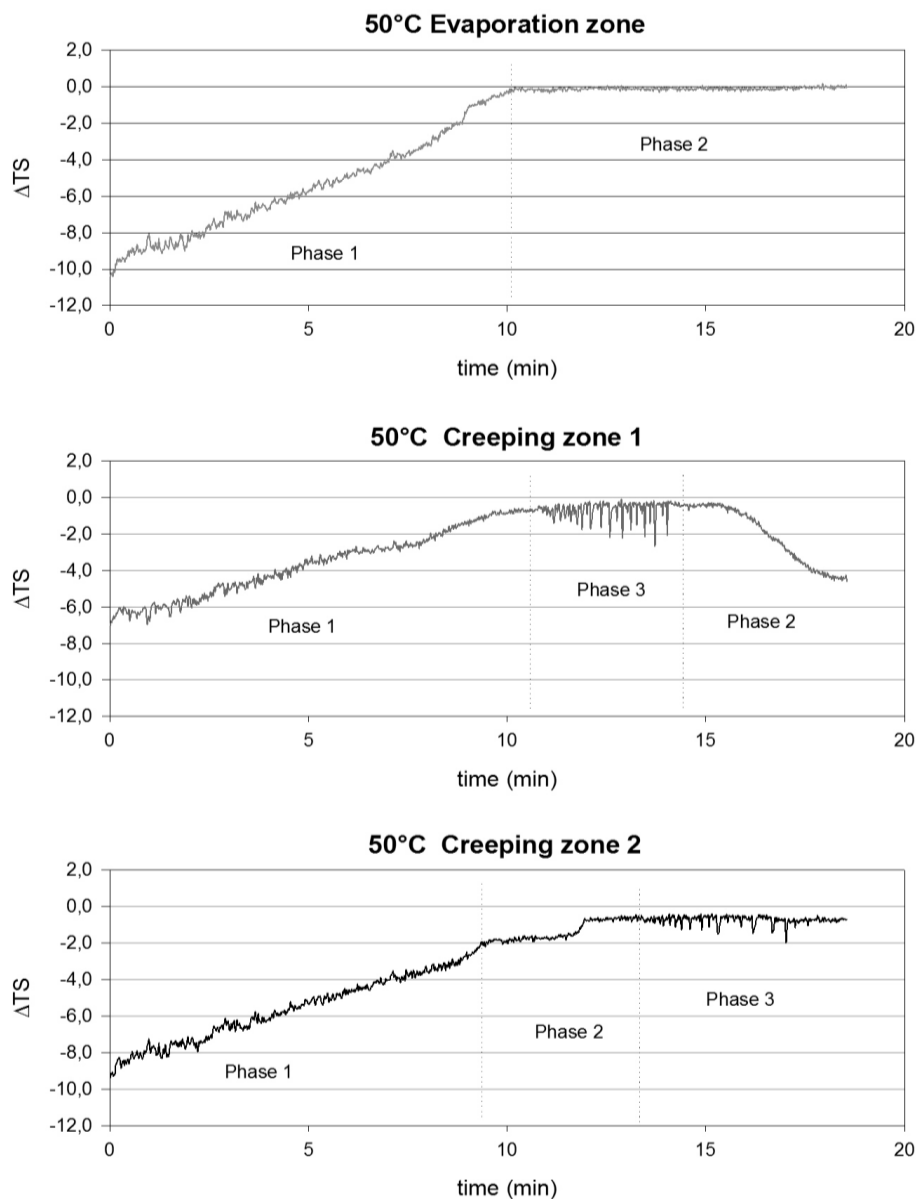


**Figure 4:** Thermosignal profiles of the crystallization sequence at 50°C. Profiles corresponded to measuring points signals in Figure 2h as EV, C1 and C2. Phase I, II and III are present. Creeping is shown as an intermittent decrease in thermosignal.



mainly due to the shape factor. During this phase I,  $\Delta TS$  decreased steadily over time (Figures 3, 4). The increase of emissivity with time was due to evaporation, which induced a decrease of the thickness of the droplets.

This homogeneous increase in thermosignal may be due to mass diffusion as a result of the first crystals formation, since sometimes, crystal germs could be distinguished in the solution edge due to their lower emissivity (Figure 2 b, f).

**Phase II: Crystal growth driven by evaporation.** This phase is featured by a higher thermosignal zone that expanded from the centre to the edges and to the growing crystals. This corresponded to water evaporation and a final visible mass diffusion from lowest concentrated areas towards the highest concentrated ones, that is the crystal surface [4]. The thermosignal profile differed depending on the measured spot.

The transition between phase I and phase II differs depending on the formation or not of visible crystals in the measured point. In areas where crystals formed, the transition from phase I to phase II is observed as a sharp increase of the thermosignal (Fig. 4) at the moment of evaporation. These abrupt increases of thermosignal had maximal values around 0.2 I.U. in the test at 25°C and 2 I.U. in the tests at 50°C. The  $\Delta TS$  after stabilization was always below zero. The thermosignal was lower, since NaCl emissivity is lower than that of the black tape [24, 25]. At 25°C, this stabilization occurred with a negative  $\Delta TS$  around 0.2-0.4 (Figure 2d, h, Figure 3) up to 1 I.U. in a few cases, depending mainly on the crystal shape. In those places where all the solution had totally dried out and were apparently devoid of crystals, the thermosignal stabilized at values similar to the black reference (around 0 I.U.) (Fig 4 top). The transition from phase I to phase II was observed to be progressive. In low concentrated droplets, the phase II marked the complete evaporation and the end of the thermal effect.

**Phase III: “Pop-cold events”.** After phase II, no more solution remained visible with the IRT. However, in medium and high concentrated droplets (14 and 26%), intermittent decreases of the thermosignal around and on the previously formed crystals were observed (Figure 3-4). These indicated that evaporation was not yet completed and stepped crystal growth processes were still occurring.

At that step, crystals were formed by creeping mechanism. Creeping is explained as the evaporation-driven extension of crystals. Hazlehurst [27] described the creeping as an intermittent process, where crystal growth is halted temporarily and more crystals grow outside the first crystal layer. The creeping crystals, formed after the first regular layer of crystals, are disposed in irregular layers in localized regions. These episodic pulses are the consequence of the release of water of crystallization at the edge of the droplet [27, 28].

Creeping leads to an intermittent process of dissolution-crystallization. A hypothesis would be that each new dissolution on the surface resulted in a decrease in thermosignal and each crystallization in an increase. Since in this study temperature remained constant during each test and NaCl crystallization is an exothermic reaction, this decrease in thermosignal depended mostly on emissivity changes. When this intermittent variation of emissivity stopped, and signal became stable again, we considered that evaporation was completed. This phenomenon may take place in several points of the droplet but not at the same time (Figure 34). The measured number of “pop-cold events” in each measuring point ranged from 1 to more than 100. The decrease in thermosignal varied between 0.5 and 5 I.U according to the concentration of the droplets and the temperature of the test. The presence of phase III, the number of events and the intensity in the variation of thermosignal are related mainly to concentration of the NaCl solution and to a lesser extent to temperature.

#### *3.5% concentration droplets.*

This low concentration permitted that crystals were formed and the evaporation/crystallization was in equilibrium. Exceptionally, in one droplet at 25 °C, an intermittent and very weak decrease in thermosignal was observed in germ crystals. However, most of the solution remained at that stage, so we cannot consider it as creeping at the scale of the study.

#### *14% concentration droplets.*

At 25°C four areas were observed and measured in one droplet and seven areas in the other one. The number of events were from 1 isolated “pop-cold event” in one of the droplets to 13 in the other one. The maximal decrease in thermosignal was of 0.5 I.U (Figure 3). At 50 °C at least twelve different points were recorded during this phase in each droplet. The areas which experimented the largest creeping showed about 20-22 “pop-cold events” with a maximum decrease of 2.50 I.U. of the thermosignal (Figure 4) and 30 events with only a decrease of 0.5 I.U. Some areas showed a low number of measured events of 6-8 and a thermosignal decrease of 0.5-1 I.U.

#### *26% concentration droplets.*

At 25°C only a few areas showed phase III, with a variable number of events, from 3 to 20. The decrease of emissivity was still less intense than at higher temperatures. At 50°C, phase III started directly without any previous phase or sometimes just after a short phase I. At the beginning of phase III, more than 30 small active areas were identified and selected to be measured. However, some of these areas joined together. The number of pop events were from 40 to 70, although there were also exceptional cases with more than 100 events. The average decrease of the thermosignal was about 4 and 5 I.U. compared to the black tape.

### 3.3 Relation between IRT signal and crystal morphology

Crystal morphologies and numbers depended on several variables such as operating conditions [29] and contact angle of the droplet with the support [30]. Clear differences in crystal size and distribution were observed in relation to salt concentration and temperature. In the study with IRT each morphology gave a different signal. Some authors [2, 29, 30] described the different morphologies observed during the crystallization of a NaCl droplet. In agreement with their observations, we found cubic crystals at the centre and the edge of the droplet. This morphology corresponded to a sequence of phases I-II, with an abrupt transition between phases, related to the crystal size. In some of the tests, efflorescences-like crystals with various morphologies grew (Figure 5). They can be formed by two mechanisms: Top-Supplied Creeping (TSC) and Bottom-Supplied Creeping (BSC). In TSC, the fresh solution necessary to the creeping process is supplied by the liquid flow aside and on top of growing crystallites, whereas in BSC, the liquid flow occurs in narrow spaces between the crystallites and the substrate [27, 28, 31]. Three different morphologies of creeping aggregates were observed by optical microscopy.

- 1) Fan-shaped crystals in contact with the substrate: in 3.5 and 14% concentrated droplets, dendritic crystals with flat fan shape that corresponded to BSC were observed. They grew from the droplet edge towards the interior and exterior of the droplet (Fig. 5 a, c). The crystallization sequence corresponded to phase I-II. This type of creeping is not observed in phase III.
- 2) Spherulite-like crystals in contact with the substrate: the crystal growth corresponded both to the BSC and TSC mechanisms because the crystal was in contact with the substrate (BSC) but also grew in height (TSC) (Fig. 5 a, d). This kind of efflorescence growth was linked to the “pop-cold events”.
- 3) Spherulite-like crystals on the surface of previous crystals: formed by hairy crystals aggregates and found mainly in medium and high concentration droplets (14 and 26%, Fig. 5 a, b, d), always corresponding to phase III “pop-cold” observations. The number and size of visible aggregates varied depending on the temperature and concentration. Figure 5 (a, d) shows that for the same concentration, spherulites are bigger at 50°C, due to the union of several spherulites to form a unique aggregate.

## 4 Conclusions

Infrared thermography (IRT) has turned out to be an appropriate technique to observe, analyze and even quantify salt crystallization. IRT allows observing “in vivo” evaporation phases and types of crystallization.

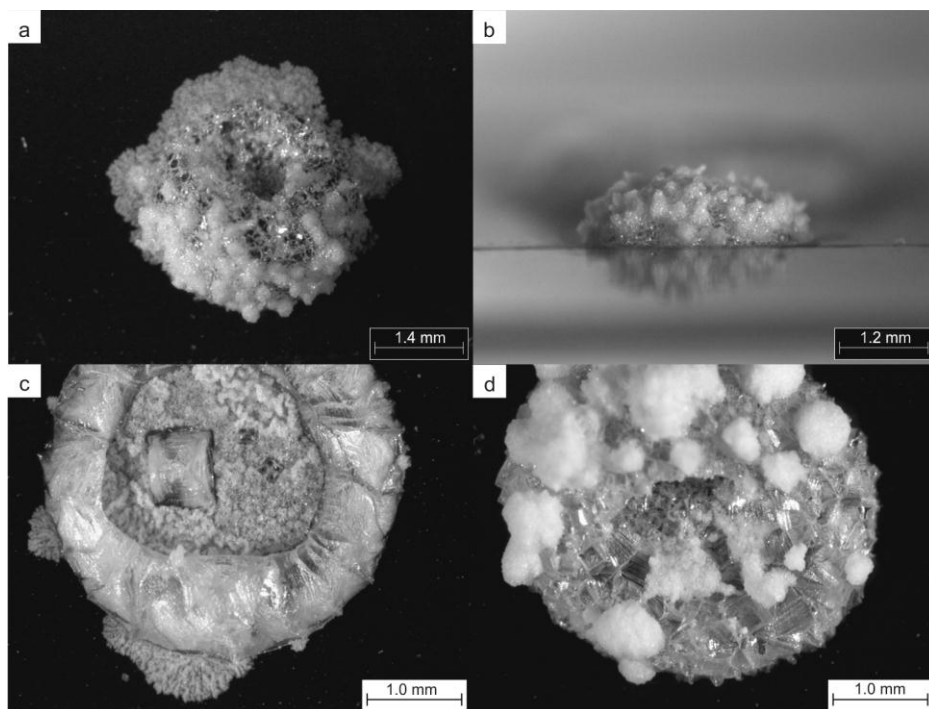


**Figure 5:** Efflorescence-like crystals. (a) and (b) 14% solution droplet crystallized at 25 °C. Small spherulite-like crystals grew on cubic crystals by TSC; (c) 14% solution droplet crystallized at 50 °C. Fan-shaped crystals grew by BSC; (d) 14% solution droplet crystallized at 50 °C. Aggregates of spherulite-like crystals grew by TSC.

In this study, different droplets of NaCl solution at different initial concentrations were dried at constant temperature (25 and 50 °C) under an IRT camera. Since temperature remained constant, in this study the thermosignal recorded depended mainly on the emissivity and was expressed as a difference compared to a reference material. Three phases were detected: (I) homogeneous evaporation and crystal nucleation, (II) crystal growth and (III) creeping. Creeping was related to the formation of efflorescence-like crystals. They may result from bottom-supplied creeping (BSC) with mainly fan shapes and found around the droplet in contact with the support or they may result from top-supplied creeping (TSC) with spherulite shape and growing on and around the precipitated crystals. TSC showed a spectacular phenomenon when recorded with IRT. It exhibited an intermittent decrease of IR thermosignal of a few seconds (called by the authors “pop-cold events”). Even if no liquid solution is visible, creeping demonstrated that evaporation was not completed and crystallization process was still occurring. At lower temperatures, creeping occurred over a longer period and decreases in thermosignal may last from several seconds up to one minute. At 50 °C

“pop-cold events” occur consecutively and are more numerous, more intense and shorter than at 25°C.

IRT is a non-destructive technique that gives information about the thermal properties of materials and their weathering degree. However, this technique is highly influenced by environmental parameters when used outdoors, and sometimes its accuracy is not enough in research field.

This study is the beginning of a wide research about saline solution behaviour studied by IRT and serves as basis for further investigations dealing with salt crystallization in porous stones and salt damage in built heritage.

## References

- [1] K. Zehnder, A. Arnold, Crystal growth in salt efflorescence, *J. Cryst. Growth* 97(2) (1989) 513-521.
- [2] C. Rodriguez-Navarro, E. Doehne, Salt weathering: influence of evaporation rate, supersaturation and crystallization pattern. *Earth Surf Proc Land*, 24(3) (1999) 191–209.
- [3] C. Rodriguez-Navarro, E. Doehne, E. Sebastian, How does sodium sulfate crystallize? Implications for the decay and testing of building materials, *Cement Concrete Res.* 30 (10) (2000) 1527–1534.
- [4] L. Pel, H. Huinink, K. Kopinga, Salt transport and crystallization in porous building materials. *Magn. Reson. Imaging*, 21(3-4) (2003) 317–320.
- [5] M. Steiger, Crystal growth in porous materials - I: The crystallization pressure of large crystals. *J. Cryst. Growth*, 282(3-4) (2005) 455–469.
- [6] E.M. Winkler, P.C. Singer, Crystallization pressure of salts in stone and concrete, *Geol Soc Am Bull*, 83 (1972) 3509-3514.
- [7] A.S. Goudie, Experimental salt weathering of limestones in relation to rock properties, *Earth Surf. Proc. Land.* 24 (1999) 715-724.
- [8] F.J. Alonso, P. Vázquez, R.M. Esbert, J. Ordaz, Ornamental granite durability: evaluation of damage caused by salt crystallization test, *Materiales de Construcción* 58 (289-290) (2008) 191-201.
- [9] P. Vázquez, A. Luque, F.J. Alonso, C.M. Grossi, Surface changes on crystalline stones due to salt crystallization. *Envir. Earth Sci.*, (2012) 1-12.

- [10] N.N. Piskunova, V.I. Rakin, Statistical analysis of dynamics of elementary processes on the surface of the growing crystal (by the AFM data), *J. Cryst. Growth*, 275(1-2), (2005) 1661–1664.
- [11] J. Dewanckele, T. De Kock, M.A. Boone, V. Cnudde, L. Brabant, M. N. Boone, G. Fronteau, L. Van Hoorebeke, P. Jacobs, 4D imaging and quantification of pore structure modifications inside natural building stones by means of high resolution X-ray CT, *Sci. Total Environ.*, 416 (2012) 436-48.
- [12] S. Bagavathiappan, B.B. Lahiri, T. Saravanan, J. Philip, J., T. Jayakumar, Infrared thermography for condition monitoring – A review, *Infrared Phys. Techn.*, 60 (2013) 35–55.
- [13] E. Grinzato, V. Vavilov, T. Kauppinen, Quantitative infrared thermography in buildings. *Energ. Buildings*, 29(1), (1998) 1–9.
- [14] H. Wiggenhauser, Active IR-applications in civil engineering. *Infrared. Phys. Techn.*, 43(3-5) (2002) 233–238.
- [15] N.P. Avdelidis, A. Moropoulou, Applications of infrared thermography for the investigation of historic structures. *J Cult Herit*, 5(1) (2004) 119–127.
- [16] A. Moropoulou, M. Kouli, N.P. Avdelidis, Infrared thermography as an NDT tool in the evaluation of materials and techniques for the protection of historic monuments. *Insight: Non-Destructive Testing and Condition Monitoring*, 42(6) (2000) 379-383.
- [17] F. Mercuri, N. Orazi, U. Zammit, S. Paoloni, M. Marinelli, P.P. Valentini, Thermographic analysis of Cultural Heritage: recent applications and perspectives, *E-preservation Sciences* 9, (2012) 84–89.
- [18] J.L. Bodnar, J.L. Nicolas, K. Mouhoubi, V. Detalle, Stimulated infrared thermography applied to thermophysical characterization of cultural heritage mural paintings. *Eur. Phys. J-Appl. Phys.* 60 (02) (2012) 21003.
- [19] M. Danese, U. Demsar, N. Masini, M. Charlton, Investigating material decay of historic buildings sing visual analytics with multi-temporal infrared thermographic data. *Archeometry*, 52, 3 (2010) 482-501.
- [20] J.L. Bodnar, J.L. Nicolas, K. Mouhoubi, J.C. Candore, V. Detalle, Characterization of an inclusion of plastazote located in an academic

- fresco by photothermal thermography, *Int. J. Thermophys.* 34 (2013) 1633-1637.
- [21] N.P. Avdelidis, A. Moropoulou, P. Theoulakis, Detection of water deposits and movement in porous materials by infrared imaging. *Infrared Phys. Techn.*, 44(3) (2003) 183–190.
- [22] C. Thomachot-Schneider, P. Vázquez, N. Lelarge, A. Conreux, C. Bouvy, M. Gommeaux, K. Mouhoubi and J.L. Bodnar. Thermal behaviour of building stones contaminated with Na<sub>2</sub>SO<sub>4</sub>. *Proceedings SWBSS2014, 3rd International Conference on Salt Weathering of Buildings and Stone Sculptures*, H. De Clercq (Ed.), (2014), 543-547
- [23] P. Vázquez, C. Thomachot-Schneider, K. Mouhoubi, G. Fronteau, M. Gommeaux, V. Barbin, J.L. Bodnar. Infrared thermography monitoring of the NaCl crystallization process. (submitted)
- [24] FLIR user manual. Series SC 655.
- [25] M. Marchetti, V. Muzet, R. Pitre, S. Datcu, L. Ibos, J. Livet, Emissivity Measurements of Road Materials, *Quantitative InfraRed Thermography Journal*, Vol 1 (1) (2004) 1.2.1-1.2.7.
- [26] S. Al-Jibbouri, J. Ulrich, The growth and dissolution of sodium chloride in a fluidized bed crystallizer. *J. Cryst. Growth*, 234 (1) (2002) 237–246.
- [27] T.H. Hazlehurst Jr, H. C. Martin, L. Brewer, The Creeping of Saturated Salt Solutions, *J. Phys. Chem.* 40.4 (1936) 439-452.
- [28] E.R. Washburn, The creeping of solutions, *J. Phys. Chem.* 31.8 (1927) 1246-1248.
- [29] H. Takiyama, T. Otsuhata, M. Matsuoka, Morphology of NaCl crystals in drowning-out precipitation operation, *Chemical Engineering Research and Design* 76.7 (1998), 809-814.
- [30] N. Shahidzadeh-Bonn, S. Rafai, Salima, D. Bonn, G. Wegdam, Salt Crystallization during Evaporation: Impact of Interfacial Properties, *Langmuir* (2008), 24, 8599-8605.
- [31] W.J.P. Van Enckevort, J.H. Los, On the Creeping of Saturated Salt Solutions. *Cryst. Growth Des.* 13(5) (2013) 1838–1848.